frontiers | Frontiers in Environmental Science

TYPE Original Research
PUBLISHED 10 February 2023
DOI 10.3389/fenvs.2023.1112522

OPEN ACCESS

EDITED BY
Rong Mao,
Jiangxi Agricultural University, China

REVIEWED BY
Zhidan Wen,
Northeast Institute of Geography and Agroecology (CAS), China
Muhua Feng,
Nanjing Institute of Geography and Limnology (CAS), China

*CORRESPONDENCE
Zhikang Wang,
wangzhikang@gzmu.edu.cn

†These authors have contributed equally to this work

SPECIALTY SECTION
This article was submitted to Freshwater Science,
a section of the journal
Frontiers in Environmental Science

RECEIVED 30 November 2022
ACCEPTED 06 January 2023
PUBLISHED 10 February 2023

CITATION
Tian L, Zhang Z, Wang Z, Zhang P, Xiong C, Kuang Y, Peng X, Yu M and Qian Y (2023), Compositional variations in algal organic matter during distinct growth phases in karst water.
Front. Environ. Sci. 11:1112522.
doi: 10.3389/fenvs.2023.1112522

Compositional variations in algal organic matter during distinct growth phases in karst water

Liye Tian[1†], Zhiwei Zhang[1†], Zhikang Wang[1,2*], Ping Zhang[1], Chao Xiong[1], Ye Kuang[3], Xingyi Peng[3], Mengxin Yu[1] and Yu Qian[1]

[1]College of Eco-Environmental Engineering, Guizhou Minzu University, Guizhou, China, [2]Guiyang Institute of Information Science and Technology, Guiyang, China, [3]Second Branch of Environmental Monitoring Station, Guiyang, China

Inland surface water plays an important role in global carbon cycling, which responds to transformation between dissolved inorganic carbon (DIC) and dissolved organic carbon (DOC). Studies have shown that algae in karst lakes and reservoirs can convert DIC to organic matter (OM) and form stable carbon sinks *via* photosynthesis. However, the pathways of conversion of inorganic carbon to organic carbon during algal growth remain unclear and need further investigation. In this study, spectroscopic techniques were applied to investigate the variations in algal organic matter (AOM) composition in the growth metabolism of *Chlorella vulgaris* and *Scenedesmus obliquus* under simulated karst water condition. The results showed that algal extracellular organic matter (EOM) contained high DIC concentration during the adaptation phase, which formed the carbon source for algal photosynthesis. In addition, DOC in algae increased after entering the stationary phase, while more OM was released into water. As algal growth proceeded, the amino groups in EOM were consumed to produce more aromatic protein-like material, while more lipid material was produced in intracellular organic matter (IOM). The spectral characterization results could intuitively determine AOM dynamics in different growth stages of algae, which can be used for establishing effective approaches for detecting organic carbon variations and responding to regional carbon cycling in karst water.

KEYWORDS

algal organic matter, karst water, carbon cycle, growth phases of algae, dissolved inorganic carbon

1 Introduction

With industrial development, a significant amount of CO_2 is emitted into the atmosphere (Kumar et al., 2011), causing a series of environmental pollution problems, eventually leading to global climate change (Rogelj et al., 2016). Recently, China has been actively pursuing the goals of achieving "peak carbon dioxide emissions" and "carbon neutrality," which will help improve the present situation of global climate change (Li et al., 2016). Global carbon cycle refers to the transformation and flow of carbon through the Earth system (atmosphere, oceans, and land) (Yang et al., 2020). As a vital part of the global carbon cycle, the biological pump mechanism was first proposed for oceans (Shackleton, 1985). Over time, studies have shown that inland water bodies (rivers, lakes, *etc.*) also manifest a critical role as a carbon source and sink in the global carbon cycle, and hard-water lakes are more advantageous in carbon sequestration (Liang and Balser, 2011). The intense biological pump effect of aquatic photosynthetic organisms in karst lakes can fix part of the carbonate weathering carbon sink flux and form a stable carbon sink (Liu and Dreybrodt, 2015).

Karst lakes and reservoirs are major surface water bodies in karst landscapes and contain high concentrations of dissolved inorganic carbon (DIC), which can provide abundant carbon for photosynthesis in aquatic organisms (Liu et al., 2010). Water systems in karst regions possess divalent ions and have a high potential for CO_2 fixation and formation of new carbonates (Lian et al., 2011). Algae are the main component of aquatic organisms in karst areas and the main carrier in carbon uptake and deposition. Nitrogen and phosphorus are essential elements required for plant growth and can influence the growth of algae (Sun H. et al., 2022). In a study of the physicochemical properties of karst lakes, it was found that the growth of karst lake algae is controlled by N and P, instead of C and P, leading to co-precipitation with calcium carbonate generated by carbon sinks (Karlsson et al., 2009). Algae involved in biological pump processes reduce the nutrient content in water, improving the environmental quality of water (Liu et al., 2008). Outbreaks of algal bloom and the release of algal organic matter (AOM) are partially mitigated by the biological pump effect (Yang et al., 2016). In addition, studies proved that karst water has a fertilizing effect and can significantly promote the growth of algae (Wang et al., 2014). Ca^{2+} and Mg^{2+} released from dolomite and limestone in karst water through carbonate dissolution can also provide additional substrates for algal growth (Zhou et al., 2022), which can utilize DIC and promote Ca^{2+} deposition, compared to algal growth in a non-karst water environment (Liu et al., 2010). Although studies on the importance of algal growth in karst lakes for the increase of carbon sinks have been widely reported (Wang et al., 2014; Liu Z. H. et al., 2018), the metabolic conversion of DIC after absorption into algae at different growth periods still remains elusive.

Spectroscopic analysis techniques, developed based on spectroscopy theory, are essential analytical tools that can be used for both qualitative and quantitative analysis (Hua et al., 2019) and are widely used in chemical, biochemical, and environmental protection applications (Liu et al., 2011). Spectroscopic characterization techniques can be used to rapidly and sensitively characterize the physicochemical characteristics of AOM and effectively reveal the composition of AOM (Hua et al., 2017). Dissolved organic carbon (DOC) serves as a key indicator for characterizing AOM because algae are critical contributors to endogenous DOC in aquatic environments (Zhang et al., 2011). The amount of aromatic compounds, proteins, *etc.*, in AOM can be effectively evaluated by using ultraviolet–visible (UV–Vis) absorption technology (Matilainen et al., 2011). Characterization of organic functional groups using Fourier transform infrared (FT-IR) spectroscopy provides a thorough understanding of the specific composition and traceability of AOM (Chu et al., 2015), and evidences of contribution from biomolecules such as proteins, lipids, and polysaccharides in algae cells are obvious (Wang Z. et al., 2012; Wang Z. K. et al., 2012). Three-dimensional fluorescence spectroscopy combined with parallel factor analysis can decipher the fluorescence information of AOM and better probe the composition and differences of AOM (Li et al., 2020). Phytoplankton discovered downstream of karst rivers produce a large amount of organic matter with the increase in the fluorescence index (Ni et al., 2020).

In this study, the metabolic conversion of DIC at different algal growth periods was investigated. Two representative algal species, *Chlorella vulgaris* and *Scenedesmus obliquus*, were selected to explore changes in organic matter at different growth periods under simulated karst water environmental conditions. EOM and intracellular organic matter (IOM) were extracted for characterization through UV–Vis absorption, FT-IR, and three-dimensional excitation and emission (3D-EEM) spectroscopy. This study aimed to reveal the *in vivo* metabolic conversion of DIC in karst lake reservoirs during the growth of algae and provide scientific support for the management of water eutrophication and the relationship between algae and carbon cycle in karst water.

2 Material and methods

2.1 Algal culture preparation

Chlorella vulgaris and *Scenedesmus obliquus* were purchased from the Freshwater Algae Bank of the Chinese Academy of Sciences. Two dominant algal species were selected based on our previous study of the distribution of dominant algal species in Aha Reservoir, a typical karst lake in Guizhou Province, southwest of China (Ge et al., 2021). Based on our previous sampling results (Zhou et al., 2022), modified BG11 medium (Supplementary Table S1, Supplementary Information) was configured to simulate the karst conditions for algae cultivation. Both algae were cultured in a light incubator (BS-2E; Wampuda, China) at 22°C ± 1°C with a light intensity of 2000 lux and a light–dark ratio of 12 h: 12 h. After algae were cultured to the logarithmic phase, the algal solution was concentrated using a centrifuge (GT10-1; Beili, China) at 4,500 r·min $^{-1}$ for spreading cultivation. Initial inoculum concentrations of *Chlorella vulgaris* and *Scenedesmus obliquus* were 2×10^6 cells·mL^{-1} and 1.65×10^6 cells·mL^{-1}, respectively, and the incubation time was 10 days. The growth cycle of the algal cells was recorded by direct counting under a microscope (UB203i; Aopu, China) using a hemocytometer plate.

2.2 Extraction of algal organic matter

EOM was extracted by the following protocol: algal supernatant was obtained by centrifugation at 8,000 r·min^{-1} for 5 min, then filtered through deionized water (18.2 MΩ cm), and pre-cleaned by filtering through 0.70 μm glass fiber paper (GF/F 47 mm; Whatman, USA) to obtain EOM (Wang et al., 2021). After EOM extraction, remaining algal cells were washed with deionized water and then centrifuged for 1 min (repeated twice), repeatedly grounded and freeze–thawed three times, and filtered *via* 0.45-μm CA membranes to obtain IOM (Pivokonsky et al., 2014). The organic carbon levels of EOM and IOM were determined using a total organic carbon analyzer (Vario TOC; Elementar, Germany).

2.3 Spectral experimental characterization

2.3.1 UV–Vis

The strength of aromaticity of AOM and the content of aromatic substances can be interpreted by $SUVA_{254}$ (Kida et al., 2018), $SUVA_{280}$ can be used to characterize proteins (Fichot and Benner, 2012), and the ratio of UVA_{210}/UVA_{254} (Sururi et al., 2020) can be used to explore the relative content of the amino structure of aromatic substances (Her et al., 2004). UV–Vis was performed after scanning the blank sample with deionized water, EOM and IOM solutions isolated from four growth periods of the two algae were subjected to a UV–Vis analyzer

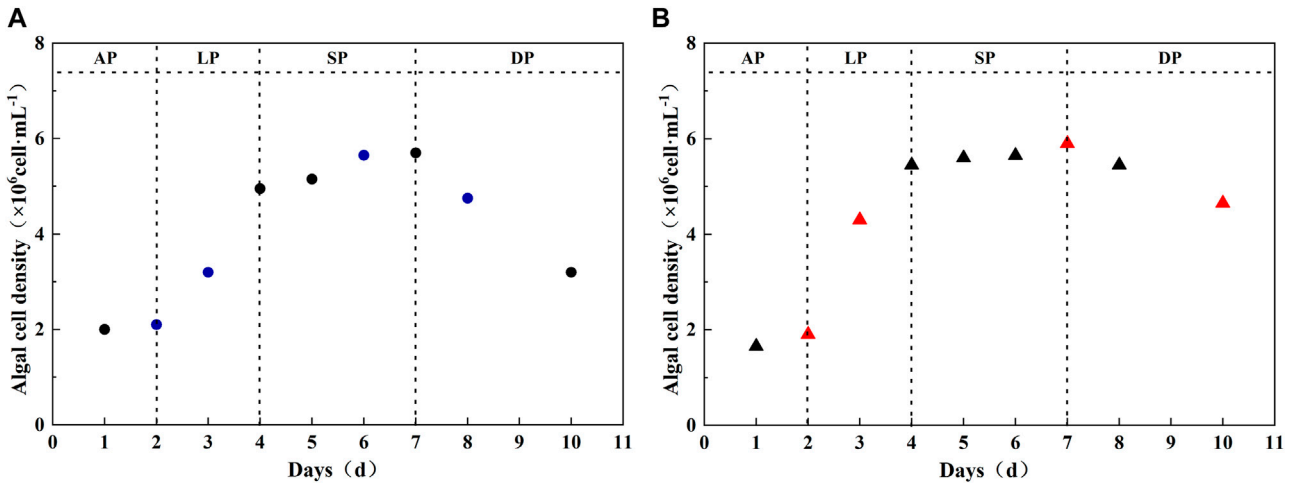

FIGURE 1
Growth curves of *Chlorella vulgaris* and *Scenedesmus obliquus* (colored points represent the characteristic days of each growth period). **(A)** *Chlorella vulgaris*; **(B)** *Scenedesmus obliquus*. AP, adaptation phase; LP, logarithmic phase; SP, stationary phase; DP, decline phase.

(UV 1800; Meixi, China) at 200–700 nm, and analysis for each sample was repeated twice.

2.3.2 FT-IR characterization

EOM and IOM solutions isolated from four growth periods of the two algae were characterized using infrared spectroscopy, and the samples were mixed with a low amount of KBr (spectrum pure; Aladdin Co., Shanghai) after being made into a dry powder using a vacuum freeze–drying machine (LGJ-12T; Songyuanhuaxin, China). All samples were compressed using a tablet press, which was further characterized by scanning using an infrared spectrometer (Nicolet 6,700, Thermo, USA), setting the scanning range to 500–3,800 cm^{-1}.

2.3.3 3D-EEM characterization

EOM and IOM solutions isolated from four growth periods of the two algae were scanned in three dimensions using a fluorescence spectrophotometer (F-380; Gangdong, China), the excitation (Ex) wavelength was set from 200 to 450 nm (interval 5.0 nm), and the emission (Em) wavelength was set from 250 to 600 nm (interval 1.0 nm), and the scanning speed, slit width, and voltage were set to 2,400 nm min^{-1}, 5.0 nm, and 700 V, respectively. Three-dimensional fluorescence parallel factor analysis (EEM-PARAFAC) was performed using MATLAB R2019b to deduct blanks and omit the interference peaks to remove the effects of Rayleigh scattering and Raman scattering (Qian et al., 2017), and the AOM model was validated by split-half analysis and residual analysis.

2.4 Data processing and statistical methods

Spectral data processing was performed using Origin 8.5 (USA). Analysis of variance at the 0.05 level and Pearson correlation analysis (at the 0.01 and 0.05 levels) were performed using SPSS 20.

3 Results and discussion

3.1 Algal culturing and DOC variation

The growth of *Chlorella vulgaris* and *Scenedesmus obliquus* in simulated karst water is shown in Figure 1. The growth cycle of algae can be divided into four stages: adaptation stage, logarithmic stage, plateau stage, and decline stage. Both *Chlorella vulgaris* and *Scenedesmus obliquus* entered the logarithmic stage of rapid growth and reproduction on the third day, but the logarithmic stage lasted for a short time. In addition, the growth of the two algae entered a stable period on days 4–7. In the stable stage, algal cells maintained a relatively stable level, the maximum algal cell concentration reached 5.7×10^6 cells·mL^{-1} and 5.9×10^6 cells·mL^{-1}, and the algae entered a period of decline on the eighth day. Results showed that the maintenance time of the stable period in the karst area was shortened, which led to the overall growth cycle being obviously shortened.

The variations in DOC values of *Chlorella vulgaris* and *Scenedesmus obliquus* are shown in Table 1. With the change in the growth cycle of the two algal species of, DOC increased significantly from the adaptation stage to the logarithmic stage. In the stable period, more cell metabolites were released in AOM, and the concentration of DOC increased. The amount of DOC in EOM was higher than that in IOM at each growth stage of *Chlorella vulgaris*, indicating that EOM would produce more DOC under the simulated condition in the karst lake reservoir. The higher DOC content in stable EOM represents more DOC accumulation with the growth of algae (Zhao et al., 2020; Ni et al., 2021). During the adaptation period, the amount of DIC was abundant and reached the maximum in EOM (20.32 ± 0.12a mg/L and 22.60 ± 0.08a mg/L). Although DIC provided the carbon source for the photosynthesis of algae, it can also be extrapolated that the biological pump effect may provide a promoting effect on the growth of algae (Supplementary Table SI2).

TABLE 1 Values of dissolved organic carbon (DOC/mg • L^{-1}) in common *Chlorella vulgaris* and *Scenedesmus obliquus* at different growth stages.

Growing period	*Chlorella vulgaris* EOM (mg•L^{-1})	*Chlorella vulgaris* IOM (mg•L^{-1})	*Scenedesmus obliquus* EOM (mg•L^{-1})	*Scenedesmus obliquus* IOM (mg•L^{-1})
Adaptation phase	5.65 ± 0.29^{c}	2.45 ± 0.03^{b}	6.93 ± 0.33^{a}	4.65 ± 0.03^{d}
Logarithmic phase	6.38 ± 0.04^{b}	2.25 ± 0.02^{b}	6.08 ± 0.04^{a}	1.98 ± 0.04^{a}
Stationary phase	8.90 ± 0.09^{a}	3.99 ± 0.00^{a}	6.61 ± 0.04^{ab}	6.85 ± 0.03^{a}
Decline phase	8.79 ± 0.07^{a}	3.74 ± 0.19^{a}	6.52 ± 0.01^{ab}	5.06 ± 0.01^{b}

$^{a–d}$: Significance analysis letter marking method, significance level: 0.01.

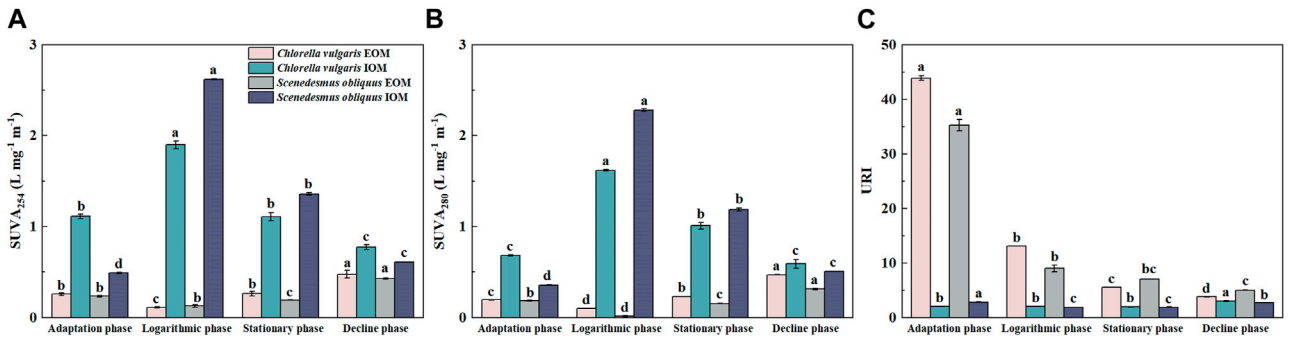

FIGURE 2
UV absorbance of *Chlorella vulgaris* and *Scenedesmus obliquus* at different growth stages. **(A)** $SUVA_{254}$; **(B)** $SUVA_{280}$; **(C)** URI.

3.2 UV–Vis determination and chemical composition analysis

The changes in $SUVA_{254}$, $SUVA_{280}$, and URI values in different growth stages of the two algae are shown in Figure 2. The $SUVA_{254}$ of logarithmic IOM for *Chlorella vulgaris* and *Scenedesmus obliquus* was 1.898 ± 0.043 L mg^{-1}·m^{-1} and 2.619 ± 0.007 L mg^{-1}·m^{-1} (Figure 2A), respectively, suggesting more aromatic substances were produced in IOM during this period (Dong et al., 2019; Sun F. et al., 2022). $SUVA_{254}$ in AOM was generally less than 1.5 L mg^{-1}·m^{-1} (Zhou et al., 2014), showing that the aromaticity of AOM was low—AOM seemed to contain less protein-like substances and organic nitrogen (Hua et al., 2018). The DOC content in EOM of both algae during all periods was higher than that in IOM, except for the stationary phase of *Scenedesmus obliquus*, but $SUVA_{254}$ in EOM was lower than that in IOM in all growth periods, showing a stronger aromatic expression in IOM under the influence of complex karst water condition (Li et al., 2012). $SUVA_{280}$ and $SUVA_{254}$ share the same trend, suggesting a potent correlation between aromaticity and protein levels (Wang et al., 2013; Liu W. et al., 2018). The $SUVA_{254}$ and $SUVA_{280}$ values in Figures 2A, B were the highest in the logarithmic phase of IOM, indicating high accumulation of aromatic compounds and proteins in the algal cells during rapid growth. However, the decrease in $SUVA_{280}$ in IOM during the decline phase may be due to the release of more organic matter outside the cell during decay of the algae (Hua et al., 2017) and higher accumulation of polysaccharides than proteins (Henderson et al., 2008). In addition, the trends of $SUVA_{254}$ and $SUVA_{280}$ in the two algae at different growth periods were completely opposite in EOM and IOM, with a gradual decrease in IOM after the logarithmic phase, indicating higher release of aromatic protein substances from cells. This was different from the results of many studies in non-karst areas (Gough et al., 2015; Chen et al., 2017). After the logarithmic phase, higher accumulation of aromatic substances in EOM than consumption was observed as $SUVA_{254}$ in EOM gradually increased.

URI values in EOM reached their highest during the adaptation period (43.877 ± 0.442a and 35.235 ± 1.059a) and gradually decreased with algal growth (Figure 2C). IOM was found to have higher URI values in the study of AOM in karst areas (Ma et al., 2022), which showed that the concentration of amino groups was higher than that of aromatic groups in EOM, and there were more proteins in EOM at the early growth stage of algae in karst lakes. The concentration of amino groups in IOM in the decline stage increased compared with that in the stable stage, which may result in the formation of unsaturated aromatic substances during the decline stage (Her et al., 2004).

3.3 Analysis of chemical components determined by FT-IR

The FT-IR spectra of EOM and IOM of the two algae at different growth periods are shown in Figure 3. The spectral peaks of EOM at 3,500–3,300 cm^{-1} indicated O-H and N-H stretching vibrations (Zhang et al., 2014), and both algae exhibited N-H stretching at 3,200–3,100 cm^{-1} during the decline phase (Ma et al., 2022). The peaks at 1700–1,600 cm^{-1} can be explained by C=O vibrations of amide I (Fawzy, 2016; Zambrano et al., 2021), while those at 1,500–1,400 cm^{-1} correspond to CH_2/CH_3 vibrations (Yang et al., 2018). Wavelength ranges of 1,200–1,100 cm^{-1} and 875 cm^{-1} show

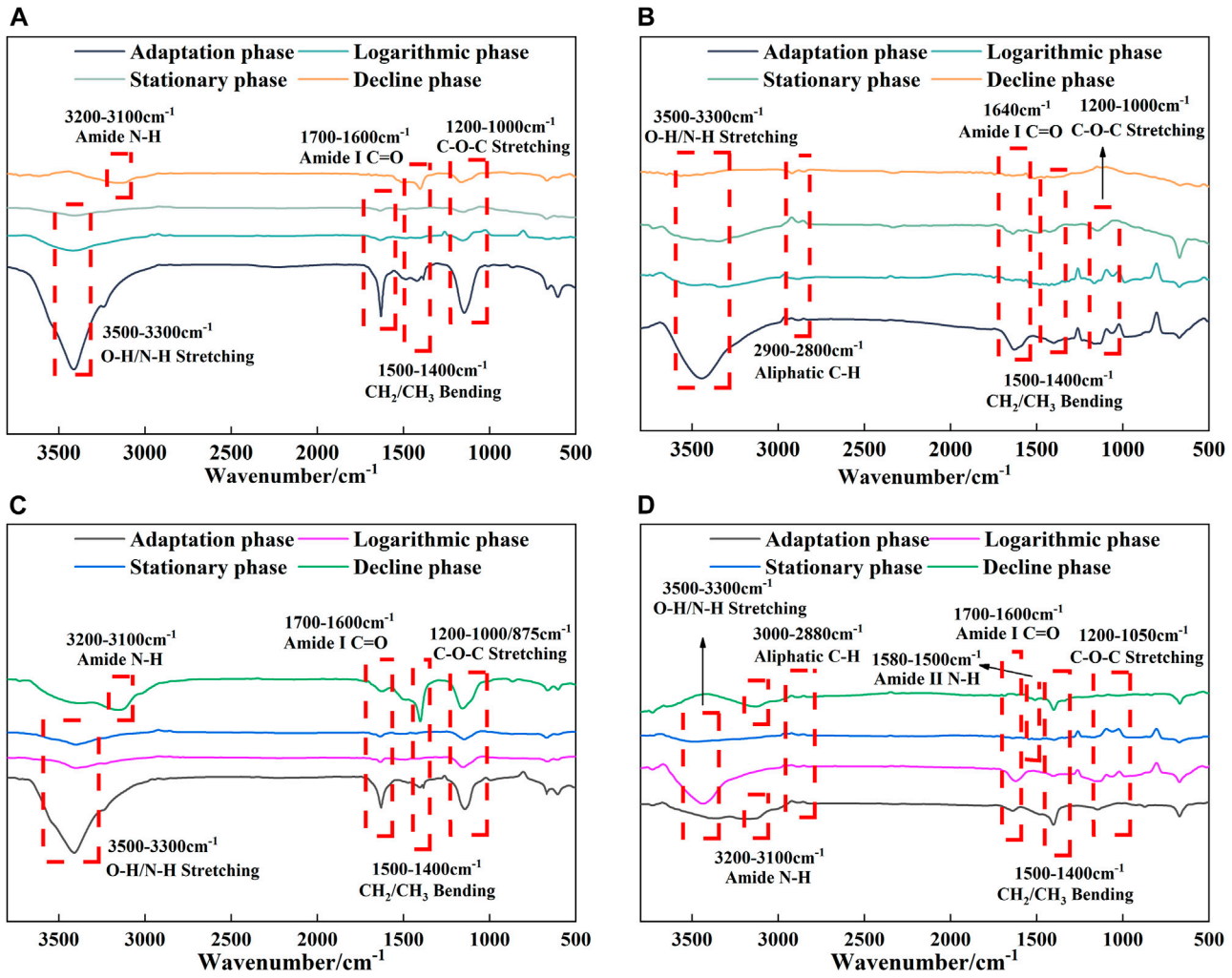

FIGURE 3
FT-IR spectra of *Chlorella vulgaris* and *Scenedesmus obliquus* at different growth stages. **(A)** *Chlorella vulgaris* EOM; **(B)** *Chlorella vulgaris* IOM; **(C)** *Scenedesmus obliquus* EOM; **(D)** *Scenedesmus obliquus* IOM.

C-O-C stretching vibrations. The peak of *Chlorella vulgaris* IOM at 3,200–3,100 cm^{-1} was not observed (Figure 3A), whereas a significant N-H stretching during the adaptation and decline phases of *Scenedesmus obliquus* was noted. In addition, C-H stretching at 3,000–2,800 cm^{-1} was observed in IOM in each growth period (Dias et al., 2021; Fawzy and Alharthi, 2021). Vibrations of amide II were also observed at 1,580–1,500 cm^{-1} in the latter two periods of *Scenedesmus obliquus* (Figure 3B; Singh et al., 2018); these peaks caused by amide groups proved the presence of proteins (Zhou et al., 2014).

The main components of both algae showed different patterns: both *Chlorella vulgaris* and *Scenedesmus obliquus* had more than 50% protein content, with lipids and polysaccharides forming 7%–24% of the main compounds (Becker, 2007; Wang et al., 2013). The obvious functional groups of proteins and polysaccharides were found at 3,500–3,300 cm^{-1} during the adaptation phase of both algal species, and the concentration of these biochemical constituents gradually decreased during the growth period. Protein peaks corresponding to 1,700–1,400 cm^{-1} similarly weakened in peak intensity after the adaptation phase, and polysaccharide peaks corresponding to 1,200–1,000/875 cm^{-1} showed a similar trend. However, the functional groups in the 3,200–3,100 cm^{-1} band were observed much frequently during the decline phase, suggesting that algal growth requires consumption of organic substances such as proteins and polysaccharides by the algal cells after the stationary phase. The peak at 3,000–2,800 cm^{-1} was more strongly expressed in IOM and can be used to explain the presence of lipids (Figure 3B). The FT-IR results revealed that both algae contain proteins and polysaccharides in EOM and IOM and that DIC promotes the production of more protein and polysaccharide material during the adaptation phase to provide energy for algal growth. The functional groups of proteins were more abundant, and as the growth of algae increased, more lipids were retained in the IOM.

3.4 3D-EEM determination of chemical composition

The 3D-EEM-PARAFAC results of EOM and IOM in *Chlorella vulgaris* and *Scenedesmus obliquus* are shown in Figure 4. All analyses

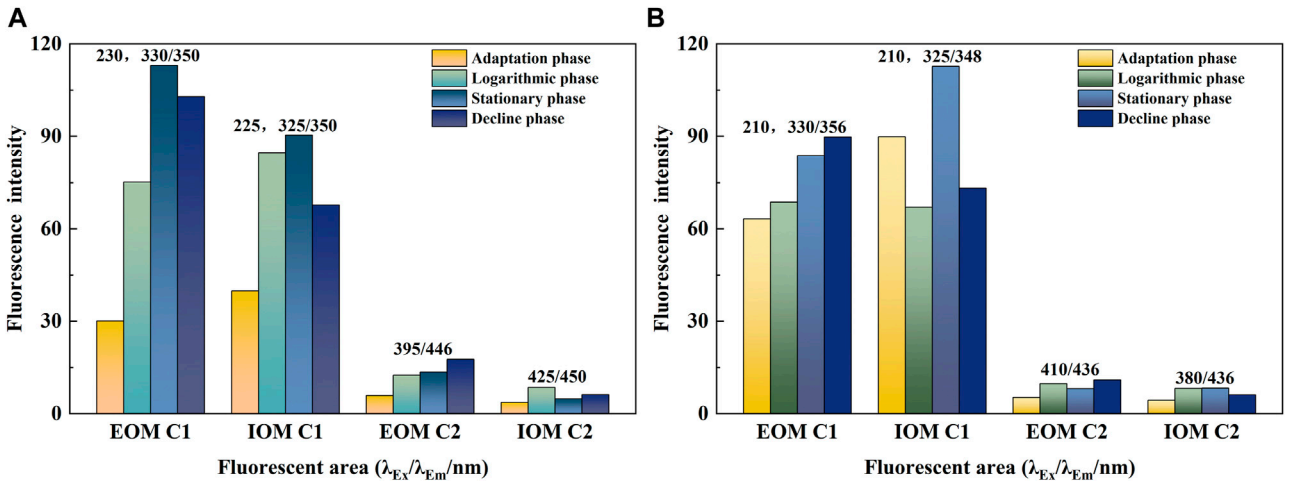

FIGURE 4
Fluorescence spectral characteristics of EOM and IOM of *Chlorella vulgaris* and *Scenedesmus obliquus* at different growth stages. **(A)** *Chlorella vulgaris*; **(B)** *Scenedesmus obliquus*.

yielded two fluorescence fractions: the C1 fraction had two excitation peaks and one emission peak, representing aromatic protein-like organic matter (AP) and soluble metabolites (SMP), respectively, and the C2 fraction for humic acid-like organic matter (HA). It was similarly found that AP and SMP were the dominant fluorescent components in AOM (Wang et al., 2021).

Although both algae showed the same fluorescence components, the fluorescence intensity differed in different periods, and the fluorescence intensity of two fluorescence components of *Chlorella vulgaris* (113.02 and 13.54) and EOM (102.89 and 17.61) increased significantly after entering the stationary phase (Figure 4A). Tryptophan-like aromatic substances, biochemical organic substances with abundant activity in algal cells, were found at 230/350 nm. This means that *Chlorella vulgaris* accumulates more protein-like substances with aromatic compounds in the AOM after entering the stationary phase (Li et al., 2012). SMP is mainly composed of tryptophan, tyrosine, and protein-like substances, and production of these substances shows that AOM is enriched in organic nitrogen and promotes the production of compounds rich in organic nitrogen (Li et al., 2012; Zhao et al., 2020). Humic acid-like substances were mainly derived from dead algal cells, and damage of algal cells was caused during grinding or freeze–thaw extraction of IOM (Zhao et al., 2020). C2 in EOM had stronger fluorescence intensity during the decline phase, and post-death, algal cells exhibited obvious humic signals. The low intensity of C2 fluorescence might be caused by powerful cell activity in the algal solution (Rochelle-Newall and Fisher, 2002).

Unlike *Chlorella vulgaris*, the C1 fraction of *Scenedesmus obliquus* had the greatest fluorescence intensity during the IOM stationary phase (112.73) (Figure 4B) and higher protein enrichment during the stationary phase, which might be driven by intracellular AOM release (Chen et al., 2017). During the decline phase, due to the death of a large quantity of algae, protein materials also decreased. Although IOM has been proven to be mainly organic nitrogen compounds with more protein aromatic substances, the soluble protein generated would be gradually broken down by the activities of algal cells (Hua et al., 2017). The highest fluorescence intensity of humic substances in the C2 fraction of *Scenedesmus obliquus* EOM was found during the decline phase (10.94), associated with the death of algae.

3.5 Correlation analysis

The spectral parameters of both algae were correlated to the chemical characteristics of AOM. In *Chlorella vulgaris* (Figures 5A, B), the correlation between DIC and TN was high (0.87 and 0.99), indicating that there was a good correlation between the accumulation of N production in algae and the change in DIC during the growth period. The correlation between DOC, DIC, and TN of *Chlorella vulgaris* and $SUVA_{254}$ and $SUVA_{280}$ showed the opposite trend in EOM and IOM, proving differences in the chemical properties of AOM, and the growth change in AOM could be better judged based on the changes in DOC, DIC, and TN. There was a high correlation between TN and URI in IOM (0.97) (Figure 5B), showing that changes in the amino-structured organic matter in IOM of *Chlorella vulgaris* can be analyzed in conjunction with the changes in TN. The correlation between DOC and C1 and C2 indicated a positive effect of organic carbon on the production of aromatic, soluble biometabolites and humic substances in EOM.

The correlations of the indices of *Scenedesmus obliquus* were slightly different from those of *Chlorella vulgaris* (Figures 5C, D). As shown in Figure 5C, DIC showed negative correlations with $SUVA_{254}$ and $SUVA_{280}$ in EOM; the differences arising between the two algae may be related to the transformation of DIC and organic matter production. The negative correlation between DIC and TN further reflected that the chemical composition and changes in EOM in *Scenedesmus obliquus* were more complex. The relationship between DOC and C1 and C2 was significantly different from that in *Chlorella vulgaris*. It is recommended to avoid using a single DOC trend for interpretation of the derivation of compositional changes in AOM (Hestir et al., 2015; Zeng et al., 2019). $SUVA_{254}$ and $SUVA_{280}$ showed an intense correlation in AOM of both algae, confirming that it is possible to discuss the analysis of aromaticity and protein content in organic matter by combining two

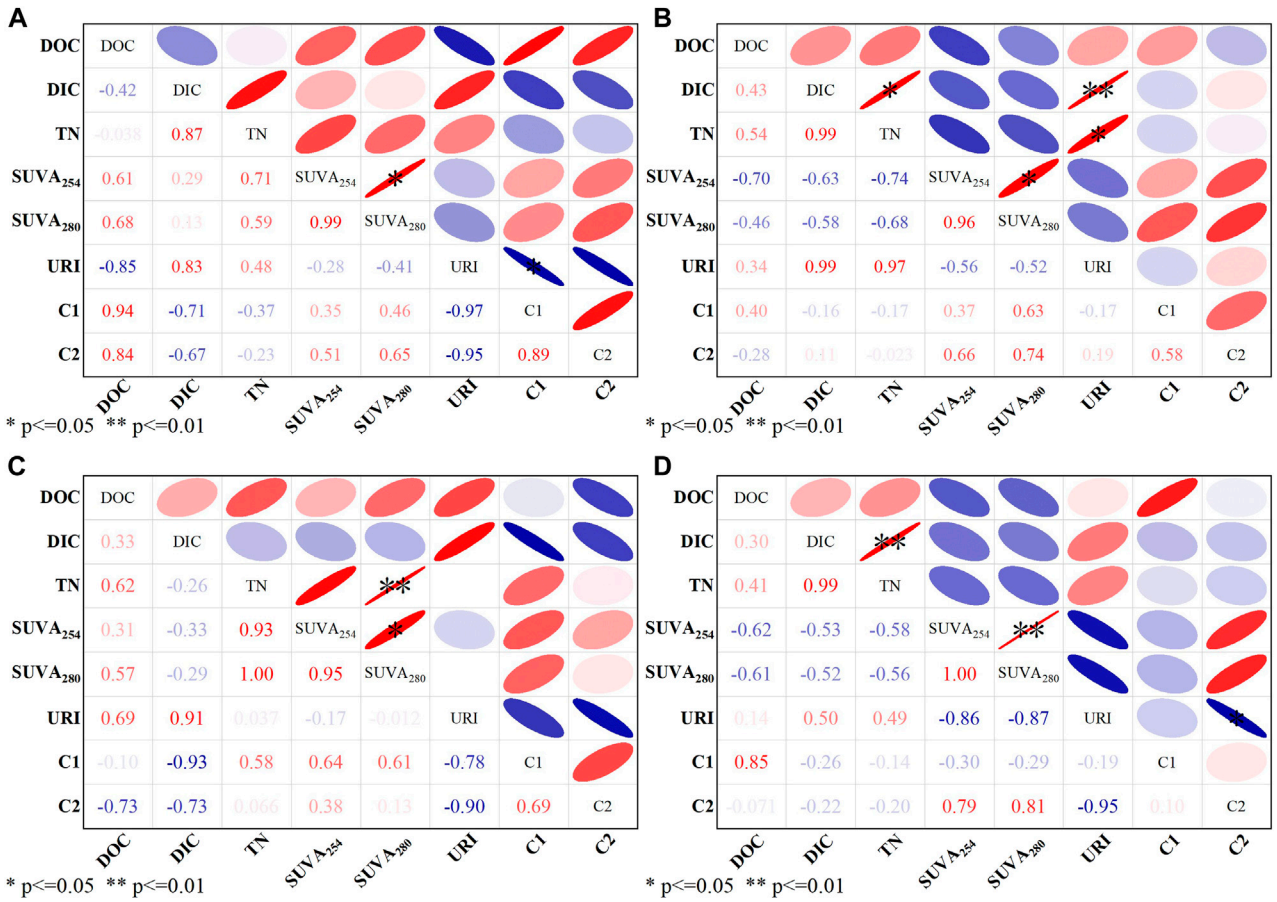

FIGURE 5
Pearson correlation analysis of spectral parameters of *Chlorella vulgaris* and *Scenedesmus obliquus*. **(A)** *Chlorella vulgaris* EOM; **(B)** *Chlorella vulgaris* IOM; **(C)** *Scenedesmus obliquus* EOM; **(D)** *Scenedesmus obliquus* IOM (n = 16).

UV coefficients (Figure 5). In addition, URI and C1 fractions were negatively correlated in both algae, and the negative correlation was more significant in EOM (Figures 5A, C), indicating that the content of amino-structured substances in EOM gradually decreased with the growth of algae. High levels of aromatic proteins (tryptophan-like substances) were produced in the algal cells, suggesting lower aromaticity in EOM. FT-IR of the adaptation phase also reflected weakening of the peak intensity of the functional groups containing amino groups, and more aromatic structure-related functional groups were generated during subsequent growth periods (Figure 3).

4 Conclusion and perspectives

In this study, we documented changes in the organic matter of *Chlorella vulgaris* and *Scenedesmus obliquus* during different growth periods under karst water conditions using various spectral characterization techniques. The conclusions of this study are as follows.

1) Both algae contained high concentrations of DIC in the EOM during the adaptation phase, and DIC provided a stable carbon source for the algae to carry out photosynthesis; the increase in DIC during the decline phase might have had a facilitating effect on the conversion of the carbon cycle.
2) More DOC would be accumulated in EOM during the stabilization and decay periods, and more organic matter was released into the water column during this period. While more aromatic compounds were generated, the aromaticity gradually decreased after the logarithmic phase of IOM.
3) IOM was found to contain more pronounced lipid functional groups. A negative correlation between URI and C1 further indicated that the amino structural material in EOM gradually decreases with the growth of algae, and more aromatic protein-like material was produced after entering the stationary phase.

In summary, the changes in DOC and DIC during the different growth periods of AOM contributed critically to the biological pump effect and accumulation of carbon sinks. By monitoring the characteristics of organic matter in AOM during different growth periods, the changes in chemical characteristics of algae involved in carbon cycle in the aquatic environment of karst areas can be determined, and the biological pump effect of aquatic ecosystems could be explored in future studies.

Data availability statement

The raw data supporting the conclusions of this article will be made available by the authors, without undue reservation.

Author contributions

LT and ZW contributed to the conception and design of the study and wrote the first draft of the manuscript. PZ organized the database. CX performed the statistical analysis. YK, XP, MY, and YQ wrote sections of the manuscript. ZW contributed to conception, funding acquisition, resources, supervision, and writing—review and editing. All authors contributed to manuscript revision and read and approved the submitted version.

Funding

This study was financially supported by the National Natural Science Foundation of China (NSFC grant Nos. 41867048, 42167050, and 42207086), the Innovation Team Project of Guizhou Higher Education ((2022)013), and the construction project of Key Laboratory of State Ethnic Affairs Commission ((2020) No. 91 of DDA office, i.e., The Karst Environmental Geological Hazard Prevention Laboratory of Guizhou Minzu University).

Conflict of interest

The authors declare that the research was conducted in the absence of any commercial or financial relationships that could be construed as a potential conflict of interest.

Publisher's note

All claims expressed in this article are solely those of the authors and do not necessarily represent those of their affiliated organizations, or those of the publisher, the editors, and the reviewers. Any product that may be evaluated in this article, or claim that may be made by its manufacturer, is not guaranteed or endorsed by the publisher.

Supplementary material

The Supplementary Material for this article can be found online at: https://www.frontiersin.org/articles/10.3389/fenvs.2023.1112522/full#supplementary-material

References

Becker, E. W. (2007). Micro-algae as a source of protein. *Biotechnol. Adv.* 25 (2), 207–210. doi:10.1016/j.biotechadv.2006.11.002

Chen, J. X., Gao, N. Y., Li, L., Zhu, M. Q., Yang, J., Lu, X., et al. (2017). Disinfection by-product formation during chlor(am)ination of algal organic matters (AOM) extracted from microcystis aeruginosa: Effect of growth phases, AOM and bromide concentration. *Environ. Sci. Pollut. Res.* 24 (9), 8469–8478. doi:10.1007/s11356-017-8515-6

Chu, H. Q., Yu, H., Tan, X. B., Zhang, Y. L., Zhou, X. F., Yang, L. B., et al. (2015). Extraction procedure optimization and the characteristics of dissolved extracellular organic matter (dEOM) and bound extracellular organic matter (bEOM) from Chlorella pyrenoidosa. *Colloids Surfaces B-Biointerfaces* 125, 238–246. doi:10.1016/j.colsurfb.2014.08.007

Dias, A., Borges, A. C., Rosa, A. P., and Martins, M. A. (2021). Green coagulants recovering Scenedesmus obliquus: An optimization study. *Chemosphere* 262, 127881. doi:10.1016/j.chemosphere.2020.127881

Dong, F. L., Lin, Q. F., Li, C., and Zhang, T. Q. (2019). Evaluation of disinfection byproduct formation from extra- and intra-cellular algal organic matters during chlorination after Fe(VI) oxidation. *RSC Adv.* 9 (70), 41022–41030. doi:10.1039/c9ra06449d

Fawzy, M. A., and Alharthi, S. (2021). Cellular responses and phenol bioremoval by green alga Scenedesmus abundans: Equilibrium, kinetic and thermodynamic studies. *Environ. Technol. Innovation* 22, 101463. doi:10.1016/j.eti.2021.101463

Fawzy, M. A. (2016). Phycoremediation and adsorption isotherms of cadmium and copper ions by Merismopedia tenuissima and their effect on growth and metabolism. *Environ. Toxicol. Pharmacol.* 46, 116–121. doi:10.1016/j.etap.2016.07.008

Fichot, C. G., and Benner, R. (2012). The spectral slope coefficient of chromophoric dissolved organic matter (S275–295) as a tracer of terrigenous dissolved organic carbon in river-influenced ocean margins. *Limnol. Oceanogr.* 57 (5), 1453–1466. doi:10.4319/lo.2012.57.5.1453

Ge, Q., Zhang, P., Ni, M., Guo, Y., Wang, Z., Hui, Z., et al. (2021). Relationships between phytoplankton and environmental factors in a typical karst plateau reservoir. *Ecol. Environ. Sci.* 30 (1), 156–164.

Gough, R., Holliman, P. J., Cooke, G. M., and Freeman, C. (2015). Characterisation of algogenic organic matter during an algal bloom and its implications for trihalomethane formation. *Sustain. Water Qual. Ecol.* 6, 11–19. doi:10.1016/j.swaqe.2014.12.008

Henderson, R. K., Baker, A., Parsons, S. A., and Jefferson, B. (2008). Characterisation of algogenic organic matter extracted from cyanobacteria, green algae and diatoms. *Water Res.* 42 (13), 3435–3445. doi:10.1016/j.watres.2007.10.032

Her, N., Amy, G., Park, H.-R., and Song, M. (2004). Characterizing algogenic organic matter (AOM) and evaluating associated NF membrane fouling. *Water Res.* 38 (6), 1427–1438. doi:10.1016/j.watres.2003.12.008

Hestir, E. L., Brando, V., Campbell, G., Dekker, A., and Malthus, T. (2015). The relationship between dissolved organic matter absorption and dissolved organic carbon in reservoirs along a temperate to tropical gradient. *REMOTE Sens. Environ.* 156, 395–402. doi:10.1016/j.rse.2014.09.022

Hua, L.-C., Lin, J.-L., Chao, S.-J., and Huang, C. (2018). Probing algogenic organic matter (AOM) by size-exclusion chromatography to predict AOM-derived disinfection by-product formation. *Sci. Total Environ.* 645, 71–78. doi:10.1016/j.scitotenv.2018.07.100

Hua, L. C., Lai, C. H., Wang, G. S., Lin, T. F., and Huang, C. P. (2019). Algogenic organic matter derived DBPs: Precursor characterization, formation, and future perspectives - a review. *Crit. Rev. Environ. Sci. Technol.* 49 (19), 1803–1834. doi:10.1080/10643389.2019.1586057

Hua, L. C., Lin, J. L., Chen, P. C., and Huang, C. P. (2017). Chemical structures of extra- and intra-cellular algogenic organic matters as precursors to the formation of carbonaceous disinfection byproducts. *Chem. Eng. J.* 328, 1022–1030. doi:10.1016/j.cej.2017.07.123

Karlsson, J., Byström, P., Ask, J., Ask, P., Persson, L., and Jansson, M. (2009). Light limitation of nutrient-poor lake ecosystems. *Nature* 460 (7254), 506–509. doi:10.1038/nature08179

Kida, M., Fujitake, N., Suchewaboripont, V., Poungparn, S., Tomotsune, M., Kondo, M., et al. (2018). Contribution of humic substances to dissolved organic matter optical properties and iron mobilization. *Aquat. Sci.* 80 (3), 26. doi:10.1007/s00027-018-0578-z

Kumar, K., Dasgupta, C. N., Nayak, B., Lindblad, P., and Das, D. (2011). Development of suitable photobioreactors for CO2 sequestration addressing global warming using green algae and cyanobacteria. *Bioresour. Technol.* 102 (8), 4945–4953. doi:10.1016/j.biortech.2011.01.054

Li, B. G., Gasser, T., Ciais, P., Piao, S. L., Tao, S., Balkanski, Y., et al. (2016). The contribution of China's emissions to global climate forcing. *NATURE* 531 (7594), 357–361. doi:10.1038/nature17165

Li, L., Gao, N., Deng, Y., Yao, J., and Zhang, K. (2012). Characterization of intracellular & extracellular algae organic matters (AOM) of Microcystic aeruginosa and formation of AOM-associated disinfection byproducts and odor & taste compounds. *Water Res.* 46 (4), 1233–1240. doi:10.1016/j.watres.2011.12.026

Li, L., Wang, Y., Zhang, W. J., Yu, S. L., Wang, X. Y., and Gao, N. Y. (2020). New advances in fluorescence excitation-emission matrix spectroscopy for the characterization of dissolved organic matter in drinking water treatment: A review. *Chem. Eng. J.* 381, 122676. doi:10.1016/j.cej.2019.122676

Lian, B., Yuan, D., and Liu, Z. (2011). Effect of microbes on karstification in karst ecosystems. *Chin. Sci. Bull.* 56 (35), 3743–3747. doi:10.1007/s11434-011-4648-z

Liang, C., and Balser, T. C. (2011). Microbial production of recalcitrant organic matter in global soils: Implications for productivity and climate policy. *Nat. Rev. Microbiol.* 9 (1), 75. doi:10.1038/nrmicro2386-c1

Liu, T., Chen, Z. L., Yu, W. Z., and You, S. J. (2011). Characterization of organic membrane foulants in a submerged membrane bioreactor with pre-ozonation using three-dimensional excitation-emission matrix fluorescence spectroscopy. *WATER Res.* 45 (5), 2111–2121. doi:10.1016/j.watres.2010.12.023

Liu, W., Zhang, L. K., Liu, P. Y., Qin, X. Q., Shan, X. J., and Yao, X. (2018). FDOM conversion in karst watersheds expressed by three-dimensional fluorescence spectroscopy. *WATER* 10 (10), 1427. doi:10.3390/w10101427

Liu, Y., Liu, Z. H., Zhang, J. L., He, Y. Y., and Sun, H. L. (2010). Experimental study on the utilization of DIC by Oocystis solitaria Wittr and its influence on the precipitation of calcium carbonate in karst and non-karst waters. *Carbonates Evaporites* 25 (1), 21–26. doi:10.1007/s13146-009-0002-9

Liu, Z. H., and Dreybrodt, W. (2015). Significance of the carbon sink produced by H2O-carbonate-CO2-aquatic phototroph interaction on land. *Sci. Bull.* 60 (2), 182–191. doi:10.1007/s11434-014-0682-y

Liu, Z. H., Macpherson, G. L., Groves, C., Martin, J. B., Yuan, D. X., and Zeng, S. B. (2018). Large and active CO2 uptake by coupled carbonate weathering. *Earth-Science Rev.* 182, 42–49. doi:10.1016/j.earscirev.2018.05.007

Liu, Z., Liu, X., and Liao, C. (2008). Daytime deposition and nighttime dissolution of calcium carbonate controlled by submerged plants in a karst spring-fed pool: Insights from high time-resolution monitoring of physico-chemistry of water. *Environ. Geol.* 55 (6), 1159–1168. doi:10.1007/s00254-007-1062-6

Ma, L., Peng, F., Dong, Q., Li, H., and Yang, Z. (2022). Identification of the key biochemical component contributing to disinfection byproducts in chlorinating algogenic organic matter. *Chemosphere* 296, 133998. doi:10.1016/j.chemosphere.2022.133998

Matilainen, A., Gjessing, E. T., Lahtinen, T., Hed, L., Bhatnagar, A., and Sillanpaa, M. (2011). An overview of the methods used in the characterisation of natural organic matter (NOM) in relation to drinking water treatment. *Chemosphere* 83 (11), 1431–1442. doi:10.1016/j.chemosphere.2011.01.018

Ni, M. F., Ge, Q. S., Li, S. Y., Wang, Z. K., and Wu, Y. J. (2021). Trophic state index linked to partial pressure of aquatic carbon dioxide in a typical karst plateau lake. *Ecol. Indic.* 120, 106912. doi:10.1016/j.ecolind.2020.106912

Ni, M. F., Jiang, S. H., and Li, S. Y. (2020). Spectroscopic indices trace spatiotemporal variability of dissolved organic matter in a river system with Karst characteristic. *J. Hydrology* 590, 125570. doi:10.1016/j.jhydrol.2020.125570

Pivokonsky, M., Safarikova, J., Baresova, M., Pivokonska, L., and Kopecka, I. (2014). A comparison of the character of algal extracellular versus cellular organic matter produced by cyanobacterium, diatom and green alga. *Water Res.* 51, 37–46. doi:10.1016/j.watres.2013.12.022

Qian, C., Wang, L. F., Chen, W., Wang, Y. S., Liu, X. Y., Jiang, H., et al. (2017). Fluorescence approach for the determination of fluorescent dissolved organic matter. *Anal. Chem.* 89 (7), 4264–4271. doi:10.1021/acs.analchem.7b00324

Rochelle-Newall, E. J., and Fisher, T. R. (2002). Production of chromophoric dissolved organic matter fluorescence in marine and estuarine environments: An investigation into the role of phytoplankton. *Mar. Chem.* 77 (1), 7–21. doi:10.1016/S0304-4203(01)00072-X

Rogelj, J., den Elzen, M., Hohne, N., Fransen, T., Fekete, H., Winkler, H., et al. (2016). Paris Agreement climate proposals need a boost to keep warming well below 2 °C. *NATURE* 534 (7609), 631–639. doi:10.1038/nature18307

Shackleton, N. J. (1985). Atmospheric carbon dioxide, orbital forcing, and climate. *Carbon cycle Atmos. CO_2 Nat. Var. Archean Present* 32, 303–317. doi:10.1029/GM032p0303

Singh, R., Upadhyay, A. K., Chandra, P., and Singh, D. P. (2018). Sodium chloride incites reactive oxygen species in green algae Chlorococcum humicola and Chlorella vulgaris: Implication on lipid synthesis, mineral nutrients and antioxidant system. *Bioresour. Technol.* 270, 489–497. doi:10.1016/j.biortech.2018.09.065

Sun, F., Ye, S., Xu, C. H., Wang, F. Y., Yu, P., Jiang, H. L., et al. (2022). Component structure and characteristic analysis of cyanobacterial organic matters. *Water Sci. Technol.* 85 (3), 789–798. doi:10.2166/wst.2022.015

Sun, H., Han, C. H., Liu, Z. H., Wei, Y., Ma, S., Bao, Q., et al. (2022). Nutrient limitations on primary productivity and phosphorus removal by biological carbon pumps in dammed karst rivers: Implications for eutrophication control. *J. Hydrology* 607, 127480. doi:10.1016/j.jhydrol.2022.127480

Sururi, M., Notodarmojo, S., Roosmini, D., Putra, P., Maulana, Y., and Dirgawati, M. (2020). An investigation of a conventional water treatment plant in reducing dissolved organic matter and trihalomethane formation potential from a tropical river water source. *J. Eng. Technol. Sci.* 52, 271–288. doi:10.5614/j.eng.technol.sci.2020.52.2.10

Wang, P., Hu, Q. J., Yang, H., Cao, J. H., Li, L., Liang, Y., et al. (2014). Preliminary study on the utilization of Ca2+ and HCO3 (-) in karst water by different sources of Chlorella vulgaris. *Carbonates Evaporites* 29 (2), 203–210. doi:10.1007/s13146-013-0170-5

Wang, X. X., Liu, B. M., Lu, M. F., Li, Y. P., Jiang, Y. Y., Zhao, M. X., et al. (2021). Characterization of algal organic matter as precursors for carbonaceous and nitrogenous disinfection byproducts formation: Comparison with natural organic matter. *J. Environ. Manag.* 282, 111951. doi:10.1016/j.jenvman.2021.111951

Wang, Z., Choi, O., and Seo, Y. (2013). Relative contribution of biomolecules in bacterial extracellular polymeric substances to disinfection byproduct formation. *Environ. Sci. Technol.* 47 (17), 9764–9773. doi:10.1021/es402067g

Wang Z., Z., Hessler, C. M., Xue, Z., and Seo, Y. (2012). The role of extracellular polymeric substances on the sorption of natural organic matter. *Water Res.* 46 (4), 1052–1060. doi:10.1016/j.watres.2011.11.077

Wang, Z. K., Kim, J., and Seo, Y. (2012). Influence of bacterial extracellular polymeric substances on the formation of carbonaceous and nitrogenous disinfection byproducts. *Environ. Sci. Technol.* 46 (20), 11361–11369. doi:10.1021/es301905n

Yang, M. X., Liu, Z. H., Sun, H. L., Yang, R., and Chen, B. (2016). Organic carbon source tracing and DIC fertilization effect in the Pearl River: Insights from lipid biomarker and geochemical analysis. *Appl. Geochem.* 73, 132–141. doi:10.1016/j.apgeochem.2016.08.008

Yang, R., Sun, H. L., Chen, B., Yang, M. X., Zeng, Q. R., Zeng, C., et al. (2020). Temporal variations in riverine hydrochemistry and estimation of the carbon sink produced by coupled carbonate weathering with aquatic photosynthesis on land: An example from the xijiang river, a large subtropical karst-dominated river in China. *Environ. Sci. Pollut. Res.* 27 (12), 13142–13154. doi:10.1007/s11356-020-07872-8

Yang, X., Zheng, X., Wu, L., Cao, X., Li, Y., Niu, J., et al. (2018). Interactions between algal (AOM) and natural organic matter (NOM): Impacts on their photodegradation in surface waters. *Environ. Pollut.* 242, 1185–1197. doi:10.1016/j.envpol.2018.07.099

Zambrano, J., García-Encina, P. A., Hernández, F., Botero-Coy, A. M., Jiménez, J. J., and Irusta-Mata, R. (2021). Removal of a mixture of veterinary medicinal products by adsorption onto a Scenedesmus almeriensis microalgae-bacteria consortium. *J. Water Process Eng.* 43, 102226. doi:10.1016/j.jwpe.2021.102226

Zeng, S., Liu, H., Liu, Z., Kaufmann, G., Zeng, Q., and Chen, B. (2019). Seasonal and diurnal variations in DIC, NO3− and TOC concentrations in spring-pond ecosystems under different land-uses at the Shawan Karst Test Site, SW China: Carbon limitation of aquatic photosynthesis. *J. Hydrology* 574, 811–821. doi:10.1016/j.jhydrol.2019.04.090

Zhang, Y. L., Yin, Y., Liu, X. H., Shi, Z. Q., Feng, L. Q., Liu, M. L., et al. (2011). Spatial-seasonal dynamics of chromophoric dissolved organic matter in Lake Taihu, a large eutrophic, shallow lake in China. *Org. Geochem.* 42 (5), 510–519. doi:10.1016/j.orggeochem.2011.03.007

Zhang, Y., Zhao, Y., Chu, H., Zhou, X., and Dong, B. (2014). Dewatering of Chlorella pyrenoidosa using diatomite dynamic membrane: Filtration performance, membrane fouling and cake behavior. *Colloids Surfaces B Biointerfaces* 113, 458–466. doi:10.1016/j.colsurfb.2013.09.046

Zhao, Z., Sun, W., Ray, A. K., Mao, T., and Ray, M. B. (2020). Coagulation and disinfection by-products formation potential of extracellular and intracellular matter of algae and cyanobacteria. *Chemosphere* 245, 125669. doi:10.1016/j.chemosphere.2019.125669

Zhou, H., Tian, L., Ni, M., Zhu, S., Zhang, R., Wang, L., et al. (2022). Effect of dissolved organic matter and its fractions on disinfection by-products formation upon karst surface water. *Chemosphere* 308, 136324. doi:10.1016/j.chemosphere.2022.136324

Zhou, S., Shao, Y., Gao, N., Deng, Y., Li, L., Deng, J., et al. (2014). Characterization of algal organic matters of Microcystis aeruginosa: Biodegradability, DBP formation and membrane fouling potential. *Water Res.* 52, 199–207. doi:10.1016/j.watres.2014.01.002